

# Self-Oscillation in Spin Torque Oscillator Stabilized by Field-like Torque

Tomohiro Taniguchi, Sumito Tsunegi, Hitoshi Kubota, and Hiroshi Imamura  
*National Institute of Advanced Industrial Science and Technology (AIST),  
 Spintronics Research Center, Tsukuba 305-8568, Japan*

(Dated: December 3, 2024)

The self-oscillation of the magnetization in a spin torque oscillator (STO) with a perpendicularly magnetized free layer and an in-plane magnetized pinned layer in the absence of an applied magnetic field was studied by numerically solving the Landau-Lifshitz-Gilbert equation. It was pointed out that field-like torque was necessary to realize stable self-oscillation in this type of STO at zero field. The numerical simulation at finite temperature showed that the presence of the field-like torque led to a high power with a relatively high oscillation frequency.

Self-oscillation of the magnetization in a nanomagnet excited by spin torque has attracted much attention for its potential application to spintronics devices such as microwave generators, magnetic sensors, and a recording and reading head of high-density hard disk drives [1–7]. Recent development on the enhancement of the perpendicular magnetic anisotropy of the CoFeB ferromagnetic layer by adding a MgO capping layer [8–10] enables us to realize a spin torque oscillator (STO) with a perpendicularly magnetized free layer and an in-plane magnetized pinned layer. It was previously shown that this type of STO produced a high emission power ( $\sim 0.5 \mu\text{W}$ ) with a narrow linewidth ( $\sim 50 \text{ MHz}$ ) by this self-oscillation [11]. It should be noted that in Ref. [11], a relatively large magnetic field (from 2 to 3 kOe) was applied to STO normal to the film plane, while the self-oscillation at zero field was interesting from a practical point of view. Although the emission power at zero field was investigated experimentally, the observed value was very low (typically, a few nW) [12].

Unfortunately, it was theoretically shown that the self-oscillation could not be excited in this type of STO in the absence of the applied field [13]. Above the critical current at which the spin torque destabilized the perpendicularly magnetized initial state, the magnetization directly moves to the anti-parallel direction with respect to the pinned layer magnetization, and stops its dynamics. This conclusion was analytically shown by calculating the energy balance between the work done by spin torque and the energy dissipation due to the damping, and was confirmed by the numerical simulation of the Landau-Lifshitz-Gilbert (LLG) equation [13].

The purpose of this letter is to show that the previous conclusion is drastically modified by taking into account the field-like torque because the presence of such torque modifies the energy balance between the spin torque and the damping. The numerical simulation of the LLG equation shows that a stable self-oscillation can be realized for a negative  $\beta$ , where  $\beta$  is the ratio between the spin torque and the field-like torque, as defined in Eq. (1) below. We also calculate the current dependences of the power and the oscillation frequency of STO at a finite temperature. The power significantly increases above the critical current when  $\beta < 0$ , whereas it rapidly decreases when  $\beta = 0$  or  $\beta > 0$ . Also, the oscillation frequency remains rela-

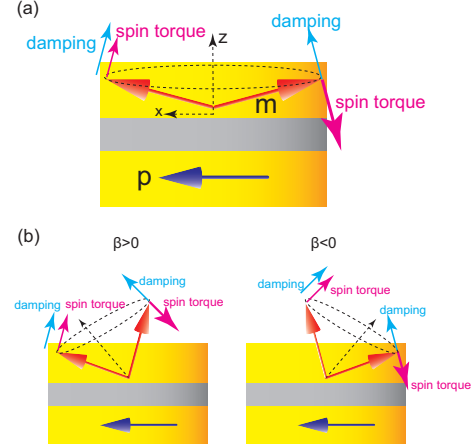


FIG. 1: (a) Schematic view of the system. The unit vectors pointing in the magnetization directions of the free and the pinned layers are denoted as  $\mathbf{m}$  and  $\mathbf{p}$ , respectively. The directions of the spin torque and the damping are indicated by the red and blue arrows, respectively. The spin torque strength near the anti-parallel alignment of  $\mathbf{m}$  and  $\mathbf{p}$  is larger than that near the parallel alignment for  $\lambda > 0$ , where  $\lambda$  is defined in Eq. (2). (b) Schematic view of the magnetization dynamics in the presence of the field-like torque with  $\beta > 0$  or  $\beta < 0$ .

tively high for  $\beta < 0$ , whereas it drops to approximately zero for  $\beta = 0$  and  $\beta > 0$ .

Figure 1 (a) schematically shows the system under consideration, where the unit vectors pointing in the magnetization directions of the free and pinned layers are denoted as  $\mathbf{m}$  and  $\mathbf{p}$ , respectively. The  $z$ -axis is normal to the film plane whereas the  $x$ -axis is parallel to the pinned layer magnetization. The current is denoted as  $I$ , where the positive current  $I > 0$  corresponds to the electrons flowing from the free layer to the pinned layer. The magnetization dynamics are described by the LLG equation [14–18],

$$\begin{aligned} \frac{d\mathbf{m}}{dt} = & -\gamma \mathbf{m} \times \mathbf{H} - \gamma H_s \mathbf{m} \times (\mathbf{p} \times \mathbf{m}) \\ & - \gamma \beta H_s \mathbf{m} \times \mathbf{p} + \alpha \mathbf{m} \times \frac{d\mathbf{m}}{dt}, \end{aligned} \quad (1)$$

where  $\gamma$  and  $\alpha$  are the gyromagnetic ratio and the Gilbert damping constant, respectively. Throughout this letter, we consider the case of the zero applied field. The mag-

netic field  $\mathbf{H} = (H_K - 4\pi M)m_z\mathbf{e}_z$  consists of the crystalline anisotropy field  $H_K$  and the demagnetization field  $4\pi M$ . Because we are interested in the perpendicularly magnetized free layer,  $H_K$  should be larger than  $4\pi M$ . The magnetic field can be defined as the derivative of the energy density  $E = -M(H_K - 4\pi M)m_z^2/2$  with respect to the magnetization  $M\mathbf{m}$ , i.e.,  $\mathbf{H} = -\partial E/\partial(M\mathbf{m})$ . The second and third terms on the right-hand side of Eq. (1) represent the spin torque and the field-like torque, respectively. The spin torque strength,

$$H_s = \frac{\hbar\eta I}{2e(1 + \lambda\mathbf{m} \cdot \mathbf{p})MV}, \quad (2)$$

consists of the volume of the free layer  $V$  and the spin torque parameters,  $\eta$  and  $\lambda$  [18], where  $\eta$  corresponds to the spin polarization of the current and  $\lambda$  determines the dependence of the spin torque strength on the relative angle between the magnetizations,  $\mathbf{m}$  and  $\mathbf{p}$ . For the positive (negative)  $\lambda$ , the spin torque magnitude near the anti-parallel alignment of  $\mathbf{m}$  and  $\mathbf{p}$  is larger than that near the parallel alignment [17], and only the positive (negative) current can excite the self-oscillation of the magnetization [2, 13].

The dimensionless parameter  $\beta$  in Eq. (1) is the ratio between the spin torque and the field-like torque. The origin of the field-like torque is the same as that of the spin torque, i.e., the transfer of the transverse spin angular momentum from the conduction electron to the free layer magnetization. While the magnitude of the field-like torque is negligible in a giant magnetoresistive (GMR) system [19, 20], in a magnetic tunnel junction (MTJ) it reaches a few tens of percents of the spin torque magnitude [21, 22]. The value of  $\beta$  has been experimentally measured by using the spin torque diode effect [23–25], although the spin torque diode effect can measure  $\beta$  below the critical current only while the self-oscillation state is realized by the current above the critical current. Both the theoretical calculation and the experimental measurement have shown that the magnitude and sign of the field-like torque depend on the material parameters, the sample thickness, and the bias voltage [19–25]. However, for simplicity,  $\beta$  in this letter is assumed to be constant with respect to the bias voltage (current). Instead, we study the magnetization dynamics for various values of  $\beta$ .

Figures 2 (a), (b), and (c) show the time evolutions of the components of  $\mathbf{m}$  obtained by numerically solving Eq. (1), in which the values of  $\beta$  are (a)  $\beta = 0$ , (b) 0.2, and (c)  $-0.2$ , respectively. The values of the parameters are  $M = 1448$  emu/c.c.,  $H_K = 20.0$  kOe,  $V = \pi \times 60 \times 60 \times 2$  nm<sup>3</sup>,  $\eta = 0.54$ ,  $\lambda = \eta^2$ ,  $I = 1.5$  mA,  $\gamma = 1.732 \times 10^7$  rad/(Oe·s), and  $\alpha = 0.005$ , respectively [8, 10, 11, 26]. By using these parameters, the critical current to destabilize the initial state for  $\beta = 0$ ,  $I_c = [4\alpha eMV/(\hbar\eta\lambda)](H_K - 4\pi M)$  [13], is estimated to be 1.2 mA. As studied in Ref. [13], in the absence of the field-like torque ( $\beta = 0$ ), the magnetization moves to the anti-parallel direction with respect to  $\mathbf{p} = \mathbf{e}_x$ , and stops its dynamics. Similarly,

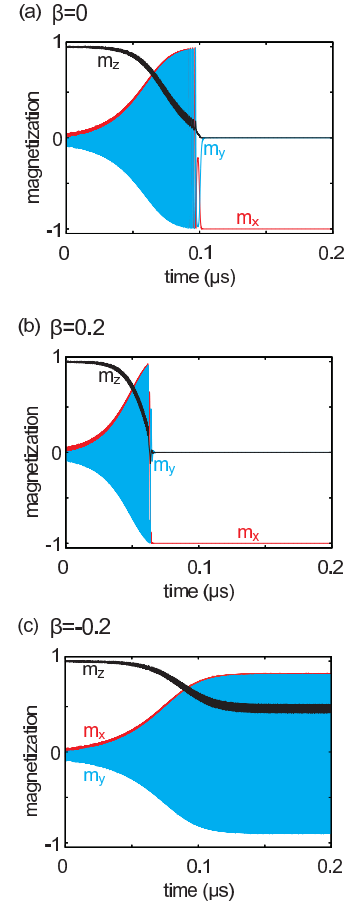


FIG. 2: The time evolutions of the components of  $\mathbf{m}$  for (a)  $\beta = 0$ , (b) 0.2, and (c)  $-0.2$ , where the red, blue, and black lines correspond to  $m_x$ ,  $m_y$ , and  $m_z$ , respectively. The current magnitude is 1.5 mA.

in the case of the positive  $\beta$ , the magnetization stops at  $\mathbf{m} = -\mathbf{p}$ . The relaxation time of the magnetization for  $\beta > 0$  is shorter than that for  $\beta = 0$ . On the other hand, stable self-oscillation is realized for negative  $\beta$ , as shown in Fig. 2 (c). The tilted angle at the self-oscillation state increases as the current increases.

The results shown in Fig. 2 indicate that the field-like torque plays a key role toward the realization of self-oscillation in this STO. In the self-oscillation state, the net energy supply by the spin torque is balanced with the energy dissipation due to the damping, and the magnetization precesses on the constant energy line. In the case of  $\beta = 0$  and  $I > 0$ , the magnetization precesses around the  $z$ -axis. It should be noted that the spin torque dissipates energy when  $m_x > 0$  because it is parallel to the damping, whereas it supplies energy when  $m_x < 0$  because it is anti-parallel to the damping, as shown in Fig. 1 (a). Because the spin torque magnitude for  $m_x < 0$  is larger than that for  $m_x > 0$  when  $\lambda > 0$ , the spin torque supplies a finite energy to the free layer. As studied in Ref. [13], in the absence of the applied field, spin torque above  $I_c$  always overcomes the damping during  $m_z = 1$  to  $m_z = 0$ , whereby self-oscillation cannot be realized. The magnetization moves to the film-plane and stops its

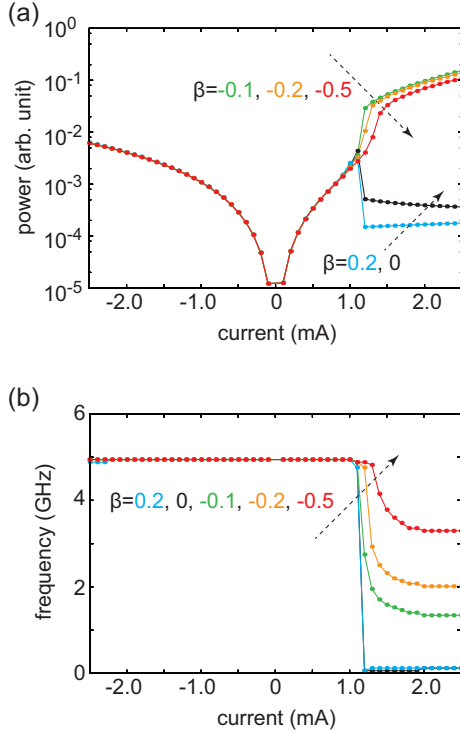


FIG. 3: Dependences of (a) the powers and (b) the oscillation frequencies of STO on the applied current, where the value of  $\beta$  varies from  $-0.5$  to  $0.2$ .

dynamics at  $\mathbf{m} = -\mathbf{p}$ . In the case of  $\beta \neq 0$ , the field-like torque acts approximately as an applied field pointing in the positive (negative)  $x$ -direction for  $\beta > 0$  ( $< 0$ ), and modifies the precession trajectory, as shown in Fig. 1 (b), due to which the amount of energy supplied by the spin torque differs from that for  $\beta = 0$ . For the positive  $\beta$ , the amount of energy supplied by the spin torque increases, and the magnetization rapidly moves to  $\mathbf{m} = -\mathbf{p}$ , as shown in Fig. 2 (b). On the other hand, for the negative  $\beta$ , the energy supplied decreases. Then, the spin torque balances with the damping above the film-plane, and therefore, the stable self-oscillation of the magnetization can be realized.

We also calculated the power and oscillation frequency of STO, both of which depend on  $m_x(t)$  through the magnetoresistance effect  $\propto \Delta R \mathbf{m} \cdot \mathbf{p}$  [11], where  $\Delta R = R_{\text{AP}} - R_{\text{P}}$  is the difference in the resistances between the parallel (P) and anti-parallel (AP) alignments of  $\mathbf{m}$  and  $\mathbf{p}$ . The power is defined as  $\int_0^\infty |m_x(f)|^2 df$  [11], where  $m_x(f)$  is the Fourier transformation of  $m_x(t)$ . The random torque,  $-\gamma \mathbf{m} \times \mathbf{h}$ , is added to the right-hand side of Eq. (1) to obtain not only the power at the self-oscillation state but also the mag-noise power. The components of the random field  $h_k$  ( $k = x, y, z$ ) satisfy the fluctuation-dissipation theorem [27],

$$\langle h_k(t) h_\ell(t') \rangle = \frac{2\alpha k_B T}{\gamma M V} \delta_{k\ell} \delta(t - t'), \quad (3)$$

where  $T$  is the temperature. The oscillation frequency is defined as the peak frequency of  $|m_x(f)|$ . The values of the parameters are those used in Fig. 2 with  $T = 300$  K. The sampling number is  $10^3$ .

Figures 3 (a) and (b) show the powers and oscillation frequencies for various  $\beta$ , respectively. Only the positive current can induce the magnetization dynamics in this system [13], and the power observed in the negative current region corresponds to the mag-noise power. We focus on the positive current region here. The most remarkable point is that the power significantly increases above the critical current ( $\simeq 1.2$  mA) for  $\beta < 0$ , whereas it decreases for  $\beta = 0$  and  $\beta > 0$ . This is because the stable self-oscillation of the magnetization can be realized in the case of  $\beta < 0$  whereas the magnetization dynamics stop at  $\mathbf{m} = -\mathbf{p}$  in the cases of  $\beta = 0$  and  $\beta > 0$ . For negative  $\beta$ , the tilted angle of the magnetization from the  $z$ -axis increases as the absolute value of  $\beta$  decreases, due to which the power for  $\beta = -0.1$  is greater than that for  $\beta = -0.5$ . For the same reasons, the oscillation frequency for  $\beta < 0$  remains relatively high compared with those for  $\beta = 0$  and  $\beta > 0$ , and the oscillation frequency for  $\beta = -0.1$  is lower than that for  $\beta = -0.5$ . In the cases of  $\beta = 0$  and  $\beta > 0$ , the powers are the mag-noise powers originated from the random oscillation of the magnetization around the  $z$ - or  $x$ -axis, depending on whether the current magnitude is below or above the critical current. Because the oscillation amplitude of  $m_x$  for the precession around the  $z$ -axis is larger than that for the precession around the  $x$ -axis, the power drops at the critical current.

In conclusion, the magnetization dynamics of STO with a perpendicularly magnetized free layer and an in-plane magnetized pinned layer was studied by numerically solving the LLG equation. We found that the field-like torque enabled the realization of a stable self-oscillation of the magnetization in this type of STO. The power and oscillation frequency of STO were calculated from the LLG equation at a finite temperature. The results also showed that the presence of the field-like torque led to a high power with a relatively high oscillation frequency.

The authors would like to acknowledge H. Maehara, A. Emura, T. Yoroazu, S. Tamaru, H. Arai, M. Konoto, K. Yakushiji, T. Nozaki, A. Fukushima, K. Ando, and S. Yuasa. This work was supported by JSPS KAKENHI Number 23226001.

- 
- [1] S. I. Kiselev, J. C. Sankey, I. N. Krivorotov, N. C. Emley, R. J. Schoelkopf, R. A. Buhrman, and D. C. Ralph, *Nature* **425**, 380 (2003).
  - [2] W. H. Rippard, M. R. Pufall, S. Kaka, S. E. Russek, and T. J. Silva, *Phys. Rev. Lett.* **92**, 027201 (2004).
  - [3] D. Houssameddine, U. Ebels, B. Delaët, B. Rodmacq, I. Firastrau, F. Ponthenier, M. Brunet, C. Thirion, J.-P. Michel, L. Prejbeanu-Buda, et al., *Nat. Mater.* **6**, 447 (2007).
  - [4] S. Bonetti, P. Muduli, F. Mancoff, and J. Akerman, *Appl. Phys. Lett.* **94**, 102507 (2009).
  - [5] K. Kudo, T. Nagasawa, K. Mizushima, H. Suto, and R. Sato, *Appl. Phys. Express* **3**, 043002 (2010).
  - [6] H. Suto, T. Nagawasa, K. Kudo, K. Mizushima, and R. Sato, *Appl. Phys. Express* **4**, 013003 (2011).
  - [7] J. Sinha, M. Hayashi, Y. K. Takahashi, T. Taniguchi, M. Drapeko, S. Mitani, and K. Hono, *Appl. Phys. Lett.* **99**, 162508 (2011).
  - [8] S. Yakata, H. Kubota, Y. Suzuki, K. Yakushiji, A. Fukushima, S. Yuasa, and K. Ando, *J. Appl. Phys.* **105**, 07D131 (2009).
  - [9] S. Ikeda, K. Miura, H. Yamamoto, K. Mizunuma, H. D. Gan, M. Endo, S. Kanai, J. Hayakawa, F. Matsukura, and H. Ohno, *Nat. Mater.* **9**, 721 (2010).
  - [10] H. Kubota, S. Ishibashi, T. Saruya, T. Nozaki, A. Fukushima, K. Yakushiji, K. Ando, Y. Suzuki, and S. Yuasa, *J. Appl. Phys.* **111**, 07C723 (2012).
  - [11] H. Kubota, K. Yakushiji, A. Fukushima, S. Tamaru, M. Konoto, T. Nozaki, S. Ishibashi, T. Saruya, S. Yuasa, T. Taniguchi, et al., *Appl. Phys. Express* **6**, 103003 (2013).
  - [12] Z. Zeng, G. Finocchio, B. Zhang, P. K. Amiri, J. A. Kantine, I. N. Krivorotov, Y. Huai, J. Langer, B. Azzerboni, K. L. Wang, et al., *Sci. Rep.* **3**, 1426 (2013).
  - [13] T. Taniguchi, H. Arai, S. Tsunegi, S. Tamaru, H. Kubota, and H. Imamura, *Appl. Phys. Express* **6**, 123003 (2013).
  - [14] E. M. Lifshitz and L. P. Pitaevskii, *Statistical Physics (part 2), course of theoretical physics volume 9* (Butterworth-Heinemann, Oxford, 1980), chap. 7, 1st ed.
  - [15] T. L. Gilbert, *IEEE Trans. Magn.* **40**, 3443 (2004).
  - [16] J. C. Slonczewski, *Phys. Rev. B* **39**, 6995 (1989).
  - [17] J. C. Slonczewski, *J. Magn. Magn. Mater.* **159**, L1 (1996).
  - [18] J. C. Slonczewski, *J. Magn. Magn. Mater.* **247**, 324 (2002).
  - [19] S. Zhang, P. M. Levy, and A. Fert, *Phys. Rev. Lett.* **88**, 236601 (2002).
  - [20] M. Zwierzycki, Y. Tserkovnyak, P. J. Kelly, A. Brataas, and G. E. W. Bauer, *Phys. Rev. B* **71**, 064420 (2005).
  - [21] I. Theodonis, N. Kioussis, A. Kalitsov, M. Chshiev, and W. H. Butler, *Phys. Rev. Lett.* **97**, 237205 (2006).
  - [22] J. Xiao and G. E. W. Bauer, *Phys. Rev. B* **77**, 224419 (2008).
  - [23] A. A. Tulapurkar, Y. Suzuki, A. Fukushima, H. Kubota, H. Maehara, K. Tsunekawa, D. D. Djayaprawira, N. Watanabe, and S. Yuasa, *Nature* **438**, 339 (2005).
  - [24] H. Kubota, A. Fukushima, K. Yakushiji, T. Nagahama, S. Yuasa, K. Ando, H. Maehara, Y. Nagamine, K. Tsunekawa, D. D. Djayaprawira, et al., *Nat. Phys.* **4**, 37 (2008).
  - [25] J. C. Sankey, Y.-T. Cui, J. Z. Sun, J. C. Slonczewski, R. A. Buhrman, and D. C. Ralph, *Nat. Phys.* **4**, 67 (2008).
  - [26] M. Konoto, H. Imamura, T. Taniguchi, K. Yakushiji, H. Kubota, A. Fukushima, K. Ando, and S. Yuasa, *Appl. Phys. Express* **6**, 073002 (2013).
  - [27] W. F. Brown Jr, *Phys. Rev.* **130**, 1677 (1963).